Editors' Suggestion | Featured in Physics

Coexistence of Nonequilibrium Density and Equilibrium Energy Distribution of Quasiparticles in a Superconducting Qubit

Thomas Connolly,[1,*,†] Pavel D. Kurilovich,[1,*,‡] Spencer Diamond,[1] Heekun Nho,[1] Charlotte G. L. Bøttcher,[1] Leonid I. Glazman,[1] Valla Fatemi,[1,2] and Michel H. Devoret[1,§]

[1]*Departments of Applied Physics and Physics, Yale University, New Haven, Connecticut 06520, USA*
[2]*School of Applied and Engineering Physics, Cornell University, Ithaca, New York 14853, USA*

(Received 21 March 2023; revised 10 August 2023; accepted 21 March 2024; published 20 May 2024)

The density of quasiparticles typically observed in superconducting qubits exceeds the value expected in equilibrium by many orders of magnitude. Can this out-of-equilibrium quasiparticle density still possess an energy distribution in equilibrium with the phonon bath? Here, we answer this question affirmatively by measuring the thermal activation of charge-parity switching in a transmon qubit with a difference in superconducting gap on the two sides of the Josephson junction. We then demonstrate how the gap asymmetry of the device can be exploited to manipulate its parity.

DOI: 10.1103/PhysRevLett.132.217001

In thermal equilibrium, the breaking of Cooper pairs in conventional superconductors should be negligible when the temperature is much smaller than the superconducting gap. Experimentally, however, a finite fraction of broken Cooper pairs, typically in the range of 10^{-9}–10^{-5}, persists to the lowest measured temperatures. While it is appreciated that the resulting "resident" quasiparticles (QPs) are detrimental for superconducting devices [1–17], their origin is not fully understood. The main conjectures are that QPs might be generated by stray millimeter-wave photons, radioactive materials, or cosmic rays [18–27].

Another long-standing mystery is the energy distribution of the resident QPs. Can the QP *energy* distribution be in thermal equilibrium with the phonon bath, despite their *density* being out of equilibrium? Previous experiments investigated this question by measuring $1e$ switching in the offset charge of a transmon qubit. These offset charge-parity switches were identified with the tunneling of resident QPs [28–30]. The authors found that the charge-parity switches are approximately equally likely to excite or relax the qubit, leading them to the conclusion that the QP energy distribution is "hot." Later, an alternative explanation for the results of [30] emerged, which does not require the resident QPs to be hot [31]. In this alternative mechanism, no preexisting QPs in the device are required to cause a parity switch. Instead, a stray photon with energy greater than 2Δ is absorbed at the Josephson junction. This process *simultaneously* breaks a Cooper pair and deposits one of the resulting quasiparticles on each side of the junction, switching the charge-parity [see Fig. 1(b)]. Further experiments [23] confirmed the prevalence of the photon-assisted parity switching mechanism in [30]. The energy distribution of the resident QPs in superconducting qubits was thus mischaracterized. To reveal it, photon-assisted parity switching must be suppressed.

Here, we suppress the rate of parity switching by stray photons to $\Gamma_0 = 0.14 \pm 0.01\ \mathrm{sec}^{-1}$ in a 3D aluminum transmon, an improvement of 3 orders of magnitude compared to a previous measurement of the same device

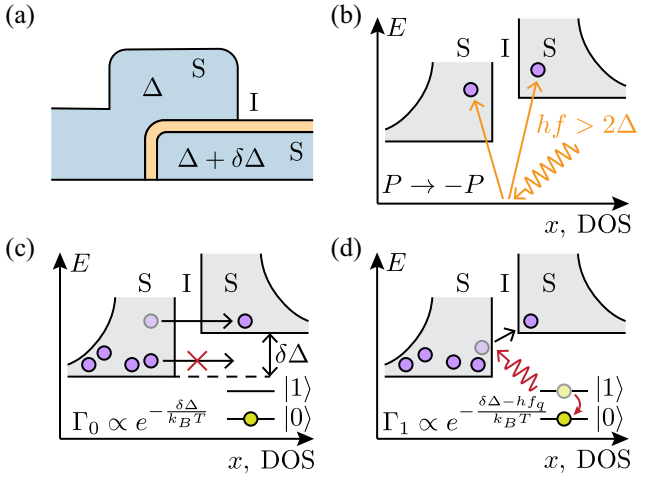

FIG. 1. (a) Schematic of the junction between two superconducting films with gaps Δ and $\Delta + \delta\Delta$. The gap difference $\delta\Delta$ arises due to the thickness difference of the films [32–34]. (b) Photon-assisted parity switching. A stray photon breaks a Cooper pair at the junction, depositing one QP on each of its electrodes and flipping the parity. This process overwhelmed the tunneling of resident QPs in Ref. [30]. (c) At small temperatures, the QP density is much higher than the value expected in thermal equilibrium, but the QP distribution function is thermalized to the temperature T of the phonon bath. As a result, when $\delta\Delta \gg k_B T$, the QP tunneling rate activates with temperature. (d) In the excited state, the qubit energy hf_q can be transferred to a QP, helping it traverse the gap difference. This reduces the activation energy by hf_q.

[35]. We achieve this by enhancing the filtering and shielding against high-frequency photons. With enhanced filtering, parity switching becomes dominated by the tunneling of resident QPs.

We observe Arrhenius activation of the parity switching rates with activation energies much smaller than the superconducting gap, which suggests that the QP energy distribution is indeed thermalized to the phonon bath, despite the nonequilibrium QP density. We attribute the activation to the difference of superconducting gaps $\delta\Delta$ between the two sides of the junction impeding QP tunneling (see Fig. 1).

The activation energies for QP tunneling are very different for the ground and excited states of the transmon. For the ground state, the activation energy is given by $\delta\Delta$ [see Fig. 1(c)]. When the transmon is excited, the QP can absorb the energy from the qubit when tunneling across the junction [see Fig. 1(d)]. This reduces the activation energy to $\delta\Delta - hf_q$, where f_q is the qubit frequency. Thus, the parity switching rate when the qubit is excited vastly exceeds the ground-state rate at low temperatures. We exploit this asymmetry to control the steady-state charge-parity of the device.

We begin by noting that monitoring of the transmon parity is allowed by the fact that parity switching effectively shifts the offset charge by $1e$. Then, if the transmon spectrum is sensitive to the offset charge, parity switching events can be detected. To attain the offset charge sensitivity, we use a transmon with a moderate ratio of Josephson and charging energies, $E_J/E_C = 17.5$. In our system, this makes the frequency pull of the resonator different for the four relevant states constituting both charge-parities for the $|0\rangle$ and $|1\rangle$ transmon states. This, along with a relatively long energy relaxation time $T_1 = 193 \pm 25$ μs and the use of a quantum-limited amplifier [36], allows us to distinguish these four states with a single-shot readout [35] at certain values of the offset charge. For the data presented in the experiment, we use $n_g = 0.163 \pm 0.003$ (in units of $2e$). At this value of offset charge, the dephasing time is $T_2^\star = 3 \pm 1$ μs.

To suppress the flux of high-frequency photons incident on the transmon, the device is placed in a shield [see Fig. 2(a)] with seams sealed by indium O-rings and interior walls coated with an absorptive carbon-impregnated epoxy. A dissipative Eccosorb CR-110 low-pass filter is placed on the microwave line inside the shield. At the minimum Cooper-pair-breaking frequency of $2\Delta/h \sim 100$ GHz, we expect [37,38] this filter to provide 35 dB of attenuation [39]. With this improved filtering, we observe much smaller parity switching rates and QP density compared to previous experiments [23,30,35]. More recent experiments have also reduced the flux of pair-breaking photons by engineering the modes of the circuit above $f = 2\Delta/h$ [40,41].

Next, we measure the parity switching rate of the qubit by collecting a series of jump traces with one measurement

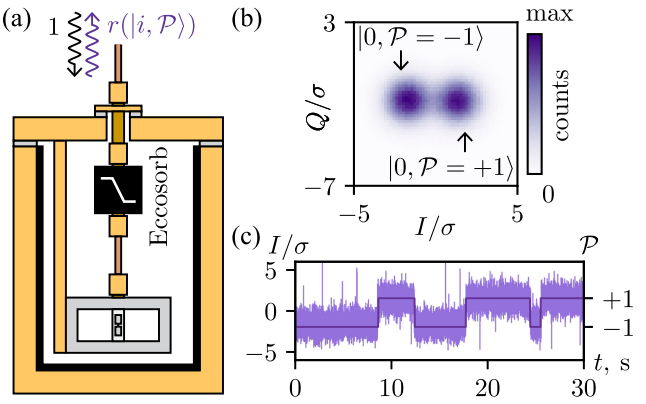

FIG. 2. Measurement of the parity switching rate in the transmon ground state. (a) Schematic of the measurement setup. 3D transmon [42,43] is placed in a light-tight shield. (b) Histogram of single-shot cavity measurements. Two distributions correspond to the ground state of the transmon in the two parity states ($\mathcal{P} = \pm 1$). (c) Measurement record of the I quadrature over a 30 sec time interval. Solid line shows a hidden Markov model state assignment.

of the qubit state every 2 ms [44]. A histogram of measurement outcomes is shown in Fig. 2(b) and a time trace is shown in Fig. 2(c). The two visible distributions correspond to the two charge parities of the transmon in the ground state. By fitting the jump traces to a hidden Markov model [45], we extract a parity switching rate of $\Gamma_0 = 0.14 \pm 0.01$ sec^{-1} [44]. Since the residual excited-state population in the described measurement is small, $\lesssim 0.2\%$, the measured Γ_0 well approximates the parity switching rate in the ground state of the transmon. We note that, in contrast to previous experiments [30,35], our excited-state population is not limited by photon-assisted parity switching.

By itself, Γ_0 is not enough to distinguish the contributions of nonequilibrium QP tunneling and photon-induced Cooper pair breaking. Therefore, we also measure the parity switching rate in the excited state of the transmon Γ_1. We do this by interleaving readout pulses played every 2 ms with variable-amplitude qubit-scrambling pulses played every 11 μs [23]. The Gaussian qubit-scrambling pulses have a standard deviation of 10 ns and lead to a steady-state excited-state population that we measure simultaneously with the parity. The resulting dependence of the parity switching rate on the excited-state population p_1 is well described by $\Gamma = (1 - p_1)\Gamma_0 + p_1\Gamma_1$ [see Fig. 3(a)]. Extrapolating this line to $p_1 = 0$ and $p_1 = 1$ yields Γ_0 and Γ_1. We obtain $\Gamma_0 = 0.14 \pm 0.01$ and $\Gamma_1 = 4.76 \pm 0.04$ sec^{-1}. Remarkably, Γ_1 is approximately 34 times higher than Γ_0. This observation is inconsistent with parity switching due to photon-induced pair breaking, which should lead to $\Gamma_0 \sim \Gamma_1$ [1,23,30,31,35]. The remaining explanation is that resident QPs dominate parity switching in the excited state.

Next, to shed light on the energy distribution of the QPs, we measure Γ_0 and Γ_1 at different temperatures

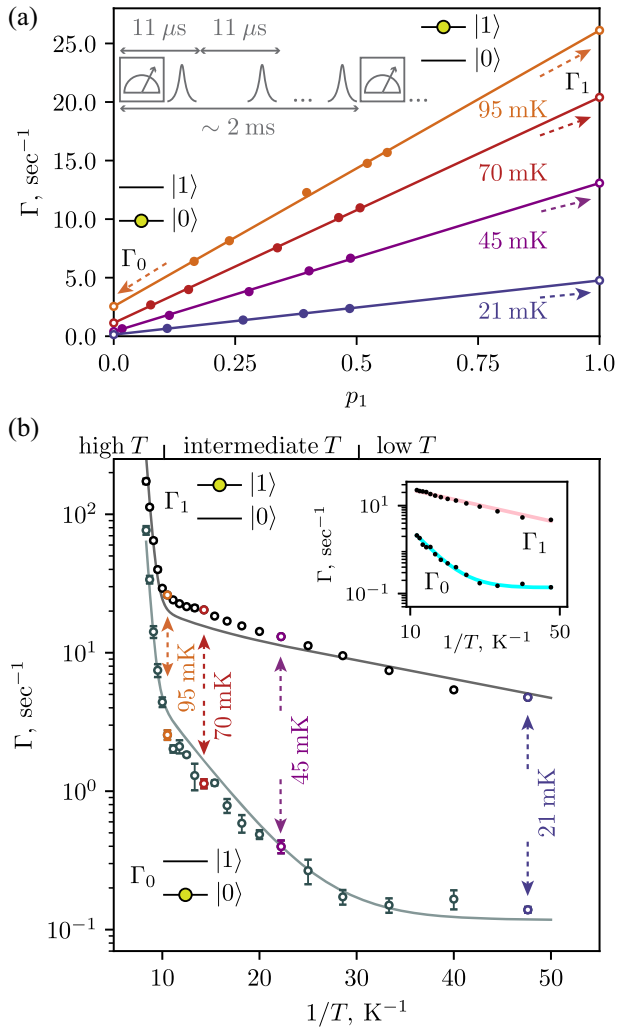

FIG. 3. Temperature dependence of the parity switching rates in the ground and excited transmon states (Γ_0 and Γ_1, respectively). Unless indicated with error bars, errors are within the size of the points. (a) Parity switching rate as a function of excited-state population p_1. Extrapolation to $p_1 = 0$ and $p_1 = 1$ yields Γ_0 and Γ_1. Different colors correspond to different mixing chamber temperatures. (b) Temperature dependence of Γ_0 and Γ_1. Solid lines show the result of a simultaneous fit of our theory to both rates (see details in the text). Inset shows the independent fit of Γ_0 and Γ_1 to an Arrhenius law in the intermediate-temperature regime. In the fits, a small offset of 0.14 sec^{-1} is added to the rates to account for the saturation of Γ_0. The difference in extracted activation energies between Γ_0 and Γ_1, $\delta E_A/h = 3.4 \pm 0.2$ GHz, is close to the qubit frequency, $f_q = 3.826$ GHz.

[see Fig. 3(b)]. The temperature dependence is distinct in three temperature regions, marked by ticks at the top of Fig. 3(b). In the high-temperature region, $T \gtrsim 100$ mK, both rates rapidly activate with activation energies $\sim h \times 50$ GHz. In the intermediate-temperature region, $30 \lesssim T \lesssim 100$ mK, rates Γ_0 and Γ_1 also thermally activate, but with much smaller activation energies. Notably, the activation energies are very different for the two qubit states. Finally, in the low-temperature region, $T \lesssim 30$ mK, Γ_0 saturates to a constant value, while Γ_1 continues to activate.

We attribute the temperature dependence of the rates to QP tunneling in the presence of gap difference at the junction. Within this model, the parity switching rates are proportional to the density of the QPs. In the low-gap film of the device, we model the QP density (normalized by the density of Cooper pairs) as

$$x_{\text{QP}} = x_{\text{QP}}^{\text{res}} + \sqrt{\frac{2\pi k_B T}{\Delta}} \exp\left(-\frac{\Delta}{k_B T}\right). \tag{1}$$

The second term describes the density of QPs in thermal equilibrium. Thermal QPs dominate x_{QP} in the high-temperature region of Fig. 3, $T \gtrsim 100$ mK, thus explaining high activation energy there. On the contrary, at $T \lesssim 100$ mK, resident QPs with a temperature-independent density $x_{\text{QP}}^{\text{res}}$ dominate x_{QP}.

To describe the data at intermediate temperatures, we calculate the QP tunneling rates in a model with different gaps at the two sides of the junction. We assume that the energy distribution of the resident QPs is in equilibrium with the phonon bath. The presence of large low-gap pads (Δ) on both sides of the junction (see Fig. S6 in Supplemental Material [44]) dictates the form of the distribution function $\mathcal{F}(\epsilon) = x_{\text{QP}}\sqrt{(\Delta/2\pi k_B T)} e^{-[(\epsilon-\Delta)/k_B T]}$ for either side at sufficiently low temperatures ($k_B T \ll \delta\Delta$). This means that the QPs in both pads primarily reside in the low-gap regions. Then, when the qubit is in the ground state, the QP tunneling rate reads

$$\Gamma_0^{\text{QP}} = \eta f_q x_{\text{QP}} \exp\left(-\frac{\delta\Delta}{k_B T}\right), \tag{2}$$

where $\eta = 4\sqrt{(E_J/E_C)(\delta\Delta/\Delta)} + \sqrt{[2\Delta/(\delta\Delta - hf_q)]}$ is a dimensionless prefactor. Here, we assumed $\delta\Delta \ll \Delta$ and $k_B T \ll \delta\Delta - hf_q$ for simplicity. To explain the origin of the activation law in Eq. (2), we note that the tunneling of QPs is suppressed while the transmon is in the ground state, since the QPs do not have enough energy to cross to the high-gap side of the junction [see Fig. 1(c)]. As the temperature is increased, a growing number of QPs have sufficient energy to tunnel, resulting in the activation of parity switching with activation energy $\delta\Delta$. This explains the behavior of Γ_0 observed in the intermediate-temperature regime of Fig. 3.

When the qubit is in the excited state, the qubit energy hf_q can be transferred to tunneling QPs, helping them overcome the gap difference [see Fig. 1(d)]. The resulting activation energy for Γ_1 becomes $\delta\Delta - hf_q$. Explicitly, we find

$$\Gamma_1^{\mathrm{QP}} = f_q \sqrt{\frac{2\Delta}{\delta\Delta - hf_q}} x_{\mathrm{QP}} \exp\left(-\frac{\delta\Delta - hf_q}{k_B T}\right). \quad (3)$$

Here, we again assumed that $\delta\Delta - hf_q \gg k_B T$ and $\delta\Delta \ll \Delta$. The difference in activation energies for Γ_1 and Γ_0 leads to large asymmetry between these rates. Equation (3) explains the behavior of Γ_1 in both the intermediate- and small-temperature regimes.

In the low-temperature region of Fig. 3, Γ_0 saturates. We attribute this to photon-assisted processes [44] because the continued activation of Γ_1 in this regime rules out elevated temperature of the resident QPs. The corresponding contributions to the parity switching rates are temperature independent and are in addition to Γ_0^{QP} and Γ_1^{QP} given by Eqs. (2) and (3). The contribution of photon-assisted processes to Γ_1 is negligible compared to QP tunneling.

Our model quantitatively matches the data. The joint fit to Γ_0 and Γ_1, shown as solid lines in Fig. 3(b), includes an extended version of the theory described in Eqs. (1)–(3) that does not require $\delta\Delta \ll \Delta$ or $\delta\Delta - hf_q \gg k_B T$ [44]. From the joint fit, we extract $\delta\Delta/h = 4.52$ GHz, $\Delta/h = 46$ GHz, and $x_{\mathrm{QP}}^{\mathrm{res}} = 5.6 \times 10^{-10}$. The extracted value of $\delta\Delta$ is close to that measured by a different method in a flux-tunable transmon of a similar design [23]. The extracted values of Δ and $\delta\Delta$ are also close to the ones expected based on the thickness of the films used in our transmon, 20 and 30 nm [32–34]. To our knowledge, our observed $x_{\mathrm{QP}}^{\mathrm{res}}$ is the smallest reported to date, which we attribute to improved filtering and shielding. Some discrepancy between the model and the data seen in Fig. 3 might arise due to the nonuniformity of superconducting gap in the films.

In addition to jointly fitting all data to our full model, we independently fit Γ_0 and Γ_1 to activation laws in the intermediate- and small-temperature regimes, as shown in the inset of Fig. 3(b). We find a difference in activation energies of $\delta E_A/h = 3.4 \pm 0.2$ GHz, close to the independently measured qubit frequency $f_q = 3.826$ GHz.

Finally, we show that the parity of the transmon can be manipulated by applying a microwave drive. This manipulation is possible because (i) the transmon frequency $f_q^{\mathcal{P}}$ depends on the charge-parity $\mathcal{P} = \pm 1$, and (ii) the parity switching rate is much higher when the transmon is in the excited state ($\Gamma_1 \gg \Gamma_0$). We note that manipulation of parity was recently reported for Andreev levels [46,47].

To explain the parity manipulation, we focus on the idealized case $\Gamma_0 = 0$. Then we show how to prepare the ground state with parity -1, assuming that initially either parity is equally probable. To bias the distribution toward -1, we drive the transmon at frequency f_q^+. The drive excites the transmon only if its ground state had parity $+1$. Subsequent relaxation may bring the transmon to the ground state with parity -1. The latter is a dark state of the drive and, therefore, the distribution becomes biased toward -1. Subsequent repetition of this process could fully polarize the system in the ground state with parity -1. Nonzero rate Γ_0 prevents full polarization, but close to unity polarization can be achieved as long as $\Gamma_1 \gg \Gamma_0$. The results of our measurements for how the degree of parity polarization depends on the strength of the driving are shown in Fig. 4.

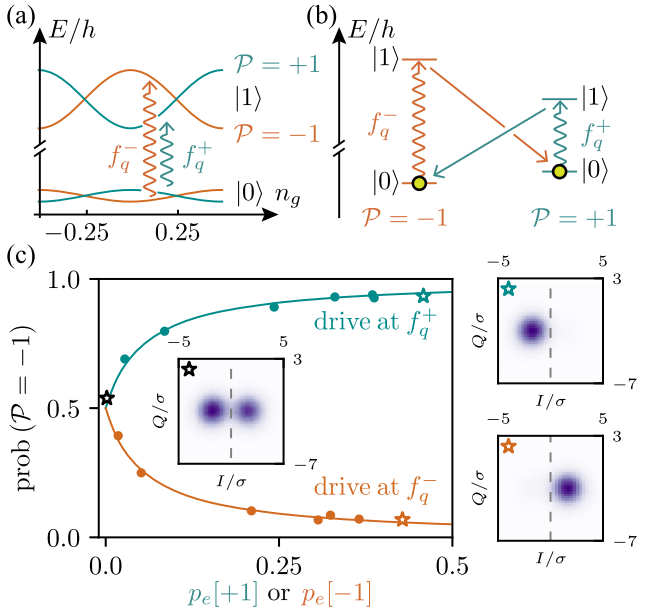

FIG. 4. Manipulation of the transmon charge-parity. The measurement is carried out at $T = 21$ mK and $n_g = 0.163$ (in units of $2e$). The pulse sequence is the same as in Fig. 3(a), except we use parity-selective 400 ns scrambling pulses. (a) Sketch of transmon energy as a function of the offset charge for $|0\rangle$ and $|1\rangle$ states with different parities, $\mathcal{P} = \pm 1$. Arrows depict the allowed transitions. (b) Since the parity switching rate in $|1\rangle$ is large, selective driving of the qubit transition for one of the parities brings the system to the ground state with the opposite parity. (c) Steady-state probability of $\mathcal{P} = -1$ as a function of the strength of driving applied at f_q^+ (teal) or f_q^- (orange). As a proxy for drive strength, we use the probability of the qubit excited state p_e conditioned on parity being $+1$ (-1). Solid lines show the fit to a detailed balance model [44]. Insets show the measurement histograms in the absence of qubit driving and in the presence of parity-selective driving.

Ability to manipulate parity can enhance qubit readout. In transmons, the readout drive has been found to cause undesired offset-charge-dependent transitions to highly excited states [48,49]. Therefore, readout might be improved by choosing the transmon parity with the lowest rate of undesired transitions.

In this Letter, we presented measurements of the charge-parity switching rates in the ground and excited states of a transmon qubit. In our device, the latter rate is dominated by the tunneling of excess resident QPs. We showed that the tunneling of nonequilibrium QPs activates with temperature (see Fig. 3). We interpret this as a consequence of

superconducting gaps being different on the two sides of the Josephson junction (see Fig. 1). Continued activation down to $T \lesssim 30$ mK implies that the QPs are well thermalized to the mixing chamber of our refrigerator, despite their out-of-equilibrium density. Therefore, although the QPs may arise from high-energy sources, rapid inelastic processes [50–52] restore their near-thermal energy distribution. Our experimental results indicate that fabricating qubits with $\delta\Delta$ larger then hf_q can suppress QP-induced decoherence [53]. Gap difference in conjunction with fast QP energy relaxation may also reduce correlated errors [20,21,24] in quantum processors resulting from QP bursts produced by ionizing radiation [19,22,23].

We acknowledge initial contributions of Kyle Serniak and Max Hays. We thank Vladislav D. Kurilovich, Manuel Houzet, Roman Lutchyn, and Rodrigo G. Cortiñas for insightful discussions. We thank Gangqiang Liu, Vidul Joshi, and Maxime Malnou for providing the parametric amplifier. We thank Alessandro Miano for the help with the measurement setup. This research was sponsored by the Army Research Office (ARO) under Grants No. W911NF-18-1-0212, No. W911NF-22-1-0053, and No. W911NF-23-1-0051, by the Air Force Office of Scientific Research (AFOSR) under Grant No. FA9550-19-1-0399, by the Office of Naval Research (ONR) under Grant No. N00014-22-1-2764, and by the U.S. Department of Energy, Office of Science, National Quantum Information Science Research Centers, Co-design Center for Quantum Advantage (C2QA) under Contract No. DE-SC0012704. The views and conclusions contained in this document are those of the authors and should not be interpreted as representing the official policies, either expressed or implied, of the U.S. Government. The U.S. Government is authorized to reproduce and distribute reprints for Government purposes notwithstanding any copyright notation herein.

*These authors contributed equally to this letter.
†tom.connolly@yale.edu
‡pavel.kurilovich@yale.edu
§michel.devoret@yale.edu

[1] L. Glazman and G. Catelani, Bogoliubov quasiparticles in superconducting qubits, SciPost Phys. Lect. Notes **31** (2021).
[2] J. Aumentado, M. W. Keller, J. M. Martinis, and M. H. Devoret, Nonequilibrium quasiparticles and 2*e* periodicity in single-Cooper-pair transistors, Phys. Rev. Lett. **92**, 066802 (2004).
[3] R. Lutchyn, L. Glazman, and A. Larkin, Quasiparticle decay rate of Josephson charge qubit oscillations, Phys. Rev. B **72**, 014517 (2005).
[4] R. M. Lutchyn, L. I. Glazman, and A. I. Larkin, Kinetics of the superconducting charge qubit in the presence of a quasiparticle, Phys. Rev. B **74**, 064515 (2006).
[5] M. D. Shaw, R. M. Lutchyn, P. Delsing, and P. M. Echternach, Kinetics of nonequilibrium quasiparticle tunneling in superconducting charge qubits, Phys. Rev. B **78**, 024503 (2008).
[6] J. M. Martinis, M. Ansmann, and J. Aumentado, Energy decay in superconducting Josephson-junction qubits from nonequilibrium quasiparticle excitations, Phys. Rev. Lett. **103**, 097002 (2009).
[7] P. J. de Visser, J. J. A. Baselmans, P. Diener, S. J. C. Yates, A. Endo, and T. M. Klapwijk, Number fluctuations of sparse quasiparticles in a superconductor, Phys. Rev. Lett. **106**, 167004 (2011).
[8] G. Catelani, R. J. Schoelkopf, M. H. Devoret, and L. I. Glazman, Relaxation and frequency shifts induced by quasiparticles in superconducting qubits, Phys. Rev. B **84**, 064517 (2011).
[9] G. Catelani, J. Koch, L. Frunzio, R. J. Schoelkopf, M. H. Devoret, and L. I. Glazman, Quasiparticle relaxation of superconducting qubits in the presence of flux, Phys. Rev. Lett. **106**, 077002 (2011).
[10] G. Catelani, S. E. Nigg, S. M. Girvin, R. J. Schoelkopf, and L. I. Glazman, Decoherence of superconducting qubits caused by quasiparticle tunneling, Phys. Rev. B **86**, 184514 (2012).
[11] P. J. de Visser, J. J. A. Baselmans, S. J. C. Yates, P. Diener, A. Endo, and T. M. Klapwijk, Microwave-induced excess quasiparticles in superconducting resonators measured through correlated conductivity fluctuations, Appl. Phys. Lett. **100**, 162601 (2012).
[12] E. Levenson-Falk, F. Kos, R. Vijay, L. Glazman, and I. Siddiqi, Single-quasiparticle trapping in aluminum nanobridge Josephson junctions, Phys. Rev. Lett. **112**, 047002 (2014).
[13] I. M. Pop, K. Geerlings, G. Catelani, R. J. Schoelkopf, L. I. Glazman, and M. H. Devoret, Coherent suppression of electromagnetic dissipation due to superconducting quasiparticles, Nature (London) **508**, 369 (2014).
[14] C. Wang, Y. Y. Gao, I. M. Pop, U. Vool, C. Axline, T. Brecht, R. W. Heeres, L. Frunzio, M. H. Devoret, G. Catelani, L. I. Glazman, and R. J. Schoelkopf, Measurement and control of quasiparticle dynamics in a superconducting qubit, Nat. Commun. **5**, 5836 (2014).
[15] F. Yan, S. Gustavsson, A. Kamal, J. Birenbaum, A. P. Sears, D. Hover, T. J. Gudmundsen, D. Rosenberg, G. Samach, S. Weber, J. L. Yoder, T. P. Orlando, J. Clarke, A. J. Kerman, and W. D. Oliver, The flux qubit revisited to enhance coherence and reproducibility, Nat. Commun. **7**, 12964 (2016).
[16] L. Grünhaupt, N. Maleeva, S. T. Skacel, M. Calvo, F. Levy-Bertrand, A. V. Ustinov, H. Rotzinger, A. Monfardini, G. Catelani, and I. M. Pop, Loss mechanisms and quasiparticle dynamics in superconducting microwave resonators made of thin-film granular aluminum, Phys. Rev. Lett. **121**, 117001 (2018).
[17] C. Kurter, C. E. Murray, R. T. Gordon, B. B. Wymore, M. Sandberg, R. M. Shelby, A. Eddins, V. P. Adiga, A. D. K. Finck, E. Rivera, A. A. Stabile, B. Trimm, B. Wacaser, K. Balakrishnan, A. Pyzyna, J. Sleight, M. Steffen, and K. Rodbell, Quasiparticle tunneling as a probe of Josephson

junction barrier and capacitor material in superconducting qubits, npj Quantum Inf. **8**, 1 (2022).
[18] A. Bespalov, M. Houzet, J. S. Meyer, and Y. V. Nazarov, Theoretical model to explain excess of quasiparticles in superconductors, Phys. Rev. Lett. **117**, 117002 (2016).
[19] A. P. Vepsäläinen, A. H. Karamlou, J. L. Orrell, A. S. Dogra, B. Loer, F. Vasconcelos, D. K. Kim, A. J. Melville, B. M. Niedzielski, J. L. Yoder, S. Gustavsson, J. A. Formaggio, B. A. VanDevender, and W. D. Oliver, Impact of ionizing radiation on superconducting qubit coherence, Nature (London) **584**, 551 (2020).
[20] J. M. Martinis, Saving superconducting quantum processors from decay and correlated errors generated by gamma and cosmic rays, npj Quantum Inf. **7**, 1 (2021).
[21] C. D. Wilen, S. Abdullah, N. A. Kurinsky, C. Stanford, L. Cardani, G. D'Imperio, C. Tomei, L. Faoro, L. B. Ioffe, C. H. Liu, A. Opremcak, B. G. Christensen, J. L. DuBois, and R. McDermott, Correlated charge noise and relaxation errors in superconducting qubits, Nature (London) **594**, 369 (2021).
[22] L. Cardani *et al.*, Reducing the impact of radioactivity on quantum circuits in a deep-underground facility, Nat. Commun. **12**, 2733 (2021).
[23] S. Diamond, V. Fatemi, M. Hays, H. Nho, P. D. Kurilovich, T. Connolly, V. R. Joshi, K. Serniak, L. Frunzio, L. I. Glazman, and M. H. Devoret, Distinguishing parity-switching mechanisms in a superconducting qubit, PRX Quantum **3**, 040304 (2022).
[24] M. McEwen *et al.*, Resolving catastrophic error bursts from cosmic rays in large arrays of superconducting qubits, Nat. Phys. **18**, 107 (2022).
[25] E. T. Mannila, P. Samuelsson, S. Simbierowicz, J. T. Peltonen, V. Vesterinen, L. Grönberg, J. Hassel, V. F. Maisi, and J. P. Pekola, A superconductor free of quasiparticles for seconds, Nat. Phys. **18**, 145 (2022).
[26] V. Iaia, J. Ku, A. Ballard, C. P. Larson, E. Yelton, C. H. Liu, S. Patel, R. McDermott, and B. L. T. Plourde, Phonon downconversion to suppress correlated errors in superconducting qubits, Nat. Commun. **13**, 6425 (2022).
[27] A. Bargerbos, L. J. Splitthoff, M. Pita-Vidal, J. J. Wesdorp, Y. Liu, P. Krogstrup, L. P. Kouwenhoven, C. K. Andersen, and L. Grünhaupt, Mitigation of quasiparticle loss in superconducting qubits by phonon scattering, Phys. Rev. Appl. **19**, 024014 (2023).
[28] D. Ristè, C. C. Bultink, M. J. Tiggelman, R. N. Schouten, K. W. Lehnert, and L. DiCarlo, Millisecond charge-parity fluctuations and induced decoherence in a superconducting transmon qubit, Nat. Commun. **4**, 1913 (2013).
[29] L. Sun, L. DiCarlo, M. D. Reed, G. Catelani, L. S. Bishop, D. I. Schuster, B. R. Johnson, G. A. Yang, L. Frunzio, L. Glazman, M. H. Devoret, and R. J. Schoelkopf, Measurements of quasiparticle tunneling dynamics in a band-gap-engineered transmon qubit, Phys. Rev. Lett. **108**, 230509 (2012).
[30] K. Serniak, M. Hays, G. de Lange, S. Diamond, S. Shankar, L. D. Burkhart, L. Frunzio, M. Houzet, and M. H. Devoret, Hot nonequilibrium quasiparticles in transmon qubits, Phys. Rev. Lett. **121**, 157701 (2018).
[31] M. Houzet, K. Serniak, G. Catelani, M. H. Devoret, and L. I. Glazman, Photon-assisted charge-parity jumps in a superconducting qubit, Phys. Rev. Lett. **123**, 107704 (2019).
[32] P. N. Chubov, V. V. Eremenko, and Y. A. Pilipenko, Dependence of the critical temperature and energy gap on the thickness of superconducting aluminum films, Sov. Phys. JETP **28**, 389 (1969).
[33] T. Yamamoto, Y. Nakamura, Y. A. Pashkin, O. Astafiev, and J. S. Tsai, Parity effect in superconducting aluminum single electron transistors with spatial gap profile controlled by film thickness, Appl. Phys. Lett. **88**, 212509 (2006).
[34] N. A. Court, A. J. Ferguson, and R. G. Clark, Energy gap measurement of nanostructured aluminium thin films for single Cooper-pair devices, Supercond. Sci. Technol. **21**, 015013 (2008).
[35] K. Serniak, S. Diamond, M. Hays, V. Fatemi, S. Shankar, L. Frunzio, R. J. Schoelkopf, and M. H. Devoret, Direct dispersive monitoring of charge parity in offset-charge-sensitive transmons, Phys. Rev. Appl. **12**, 014052 (2019).
[36] N. E. Frattini, V. V. Sivak, A. Lingenfelter, S. Shankar, and M. H. Devoret, Optimizing the nonlinearity and dissipation of a SNAIL parametric amplifier for dynamic range, Phys. Rev. Appl. **10**, 054020 (2018).
[37] M. Halpern, H. P. Gush, E. Wishnow, and V. D. Cosmo, Far infrared transmission of dielectrics at cryogenic and room temperatures: Glass, Fluorogold, Eccosorb, Stycast, and various plastics, Appl. Opt. **25**, 565 (1986).
[38] S. Danilin, J. Barbosa, M. Farage, Z. Zhao, X. Shang, J. Burnett, N. Ridler, C. Li, and M. Weides, Engineering the microwave to infrared noise photon flux for superconducting quantum systems, Eur. Phys. J. Quantum Technol. **9**, 1 (2022).
[39] The disadvantage of our filter is ∼13 dB of insertion loss at the readout frequency. This required a long 11 μs readout pulse to achieve a single-shot readout, which is still possible because $T_1 = 193 \pm 25$ μs for our qubit.
[40] X. Pan, Y. Zhou, H. Yuan, L. Nie, W. Wei, L. Zhang, J. Li, S. Liu, Z. H. Jiang, G. Catelani, L. Hu, F. Yan, and D. Yu, Engineering superconducting qubits to reduce quasiparticles and charge noise, Nat. Commun. **13**, 7196 (2022).
[41] C.-H. Liu, D. C. Harrison, S. Patel, C. D. Wilen, O. Rafferty, A. Shearrow, A. Ballard, V. Iaia, J. Ku, B. L. T. Plourde, and R. McDermott, Quasiparticle poisoning of superconducting qubits from resonant absorption of pair-breaking photons, arXiv:2203.06577.
[42] J. Koch, T. M. Yu, J. Gambetta, A. A. Houck, D. I. Schuster, J. Majer, A. Blais, M. H. Devoret, S. M. Girvin, and R. J. Schoelkopf, Charge-insensitive qubit design derived from the Cooper pair box, Phys. Rev. A **76**, 042319 (2007).
[43] H. Paik, D. I. Schuster, L. S. Bishop, G. Kirchmair, G. Catelani, A. P. Sears, B. R. Johnson, M. J. Reagor, L. Frunzio, L. I. Glazman, S. M. Girvin, M. H. Devoret, and R. J. Schoelkopf, Observation of high coherence in Josephson junction qubits measured in a three-dimensional circuit QED architecture, Phys. Rev. Lett. **107**, 240501 (2011).
[44] See Supplemental Materials at http://link.aps.org/supplemental/10.1103/PhysRevLett.132.217001 for details of our setup, measurement, data analysis, and theory.

[45] J. Schreiber, Pomegranate: Fast and flexible probabilistic modeling in PYTHON, J. Mach. Learn. Res. **18**, 1 (2018), https://jmlr.org/papers/v18/17-636.html.

[46] J. Wesdorp, L. Grünhaupt, A. Vaartjes, M. Pita-Vidal, A. Bargerbos, L. Splitthoff, P. Krogstrup, B. Van Heck, and G. De Lange, Dynamical polarization of the fermion parity in a nanowire Josephson junction, Phys. Rev. Lett. **131**, 117001 (2023).

[47] N. Ackermann, A. Zazunov, S. Park, R. Egger, and A. L. Yeyati, Dynamical parity selection in superconducting weak links, Phys. Rev. B **107**, 214515 (2023).

[48] D. Sank *et al.*, Measurement-induced state transitions in a superconducting qubit: Beyond the rotating wave approximation, Phys. Rev. Lett. **117**, 190503 (2016).

[49] M. Khezri *et al.*, Measurement-induced state transitions in a superconducting qubit: Within the rotating wave approximation, Phys. Rev. Appl. **20**, 054008 (2023).

[50] S. B. Kaplan, C. C. Chi, D. N. Langenberg, J. J. Chang, S. Jafarey, and D. J. Scalapino, Quasiparticle and phonon lifetimes in superconductors, Phys. Rev. B **14**, 4854 (1976).

[51] Y. Savich, L. Glazman, and A. Kamenev, Quasiparticle relaxation in superconducting nanostructures, Phys. Rev. B **96**, 104510 (2017).

[52] G. Catelani and D. Basko, Non-equilibrium quasiparticles in superconducting circuits: Photons vs phonons, SciPost Phys. **6**, 013 (2019).

[53] G. Marchegiani, L. Amico, and G. Catelani, Quasiparticles in superconducting qubits with asymmetric junctions, PRX Quantum **3**, 040338 (2022).